Modeling of diffusion and chemical reactions in ion-exchange resins during swelling and shrinking

Tuomo Sainio[*] *and Erkki Paatero, Lappeenranta University of Technology,*
Laboratory of Industrial Chemistry, Skinnarilankatu 34, FIN-53850 Lappeenranta, Finland

[*] *Corresponding author. E-mail: tuomo.sainio@lut.fi, Tel: +358-5-6212269,*
fax: +358-5-6212199

Abstract

Ion-exchange resins used in chromatographic separation, ion exchange, and heterogeneous catalysis are elastic polymeric materials. The extent of swelling of the polymer, and thus the dimensions of resin particles, change in response to changes in, for example, the solvent composition and salt content of the surrounding liquid. This is reflected to the intraparticle mass transfer rates through the mesh width of the apertures in the polymer network.

Mass transfer and chemical reactions in sulfonated PS–DVB ion exchange resins during shrinking and swelling of the particles were investigated experimentally and with computer simulations. A specially constructed flow-through cell and an optical microscope were used to monitor the diffusion induced volume changes of resin particles.

The applicability of particle diffusion models based on the Fick's law and the Maxwell–Stefan approach, as well as two-point approximations of these, was investigated. In the Maxwell–Stefan approach, the chemical potentials of the mobile species were calculated with models derived from thermodynamics of polymer solutions and gels by taking into account the elastic nature of the polymer. The effect of swelling ratio on the diffusion coefficients was described with a geometric obstruction model for the sake of simplicity. The governing equations were written and solved in polymer mass coordinates, which enables faster and more accurate numerical solution.

The choice of the mass transfer model was found to have a large impact on the predicted swelling behavior of the resins. It was shown that, owing to the elastic nature of the resins, diffusion coupled with volume changes of particles was best described with a model that explicitly takes the presence of the cross-links in the polymer into account.

Introduction

Several approaches to modeling diffusion of solvents in cross-linked polymers have been presented in the literature. The essence of the Tanaka–Fillmore approach [1, 2] is that liquids do not diffuse into the polymer network but the polymer network diffuses into a stagnant fluid. The diffusion coefficient of the polymer network is defined using the bulk modulus of the network and a solvent–polymer friction coefficient. The present work focuses on diffusion-induced swelling of gels in liquid mixtures with two or more components. To the best of our

knowledge, the Tanaka–Fillmore approach has not been extended to such systems, and only models describing penetration of liquids into the polymer network are considered in this work.

In rigorous treatments of the problem [3 – 5], the presence of the cross-links, and the resulting limited expansibility of the polymer network, is accounted for by introducing stress tensors in the equations of motion. Consequently, the volumetric flux into a volume element of the particle is reduced if it results in an increase in the stress of the polymer network. An alternative way is to embed the effect of the cross-links into the driving force via the solvent activity [6], which depends on the extent of swelling.

Diffusion in gel-type ion-exchange resins is analyzed in this study by using two simplified approaches (*i.e.*, without solving the equations of motion): Fick's law and the generalized Maxwell–Stefan formalism. Mass balance equations are given for spherical particles. The local swelling ratio, and hence the volume of the particle, is allowed to change with time. The mass transfer rates depend strongly on the polymer volume fraction and this effect is included by means of a simple obstruction model. In addition, simplified methods for calculating the average concentration in a particle as a function of time without solving the partial differential equation system are presented. The applicability of these models in describing swelling and shrinking rates of ion-exchange resin particles is discussed.

Materials and methods

A sulfonated, gel-type poly(styrene-co-divinylbenze) resin CS16G (Finex Oy, Finland) was used in the H^+ form. The resin has a cross-link density of 8 wt-%, and an ion-exchange capacity of 5.2 equiv/g. Deionized water and reagent grade acetic acid were used as the liquid components.

The swelling and shrinking kinetics of the resins in response to changes in the composition of the surrounding liquid were monitored in a specially constructed flow-through cell. The volume of the cell was approximately 0.1 cm^3, and the volumetric flow rate of the solvent mixture was typically 6.0 cm^3 min^{-1}. All experiments were performed at room temperature. One or more resin beads was preconditioned in a solvent mixture and placed in the cell. A step change was made in the solvent composition, and the resulting swelling or shrinking process was recorded with a digital camera through an optical microscope. The sampling rate was between 1 and 30 seconds, depending on the rate of the volume change of the particle. The particle sizes were determined off-line by using image analysis.

The shrinking kinetics measurements were started from water-swollen resin. After the new equilibrium state was reached, the swelling kinetics experiments were performed by displacing the aqueous acetic acid solution in the cell with water.

Model development

Coordinate system

Polymer mass coordinates were chosen as the frame of reference in the calculations [5, 7]. In this coordinate system, the mass of the dry polymer increases linearly along the

coordinate axis. If the location of a calculation element is defined with respect to the mass coordinate system, it remains fixed although the volume of the particle, and that of the calculation element, may change. Mathematically, the transformation between the two coordinate systems is defined through the differential operators as shown in Eq. (1).

$$\frac{\partial W}{\partial R} = \frac{A(W)\,\rho_{\mathrm{m}}}{\theta(W)} \tag{1}$$

The mass coordinate system has also another property that is of practical importance: when finite-difference methods with equidistant grid spacing are used for spatial discretization of the resulting partial differential equation system, the grid points in the mass-coordinate system are automatically concentrated in the vicinity of the particle surface. It is this region where the steepest concentration gradients are to be expected, and a denser grid improves computational accuracy and stability. Since a smaller number of grid points is required, the numerical solution is also faster.

Fickian diffusion model

In the mass coordinate system, the differential material balance describing the Fickian diffusion becomes as shown in Eqs. (2) and (3), where θ is the local swelling ratio and ρ_{m} is the density of the polymer. The numerical value of the diffusion coefficient is not affected by the coordinate transformation. It should be noted, however, that the assumption of negligible molar average velocity of the mixture with respect to the coordinate system has not been removed. When practical is preferred to rigorous, Eqs. (2) and (3) can be used as an approximation even for concentrated solutions and multicomponent systems.

$$\frac{\partial C_i^{\mathrm{S}}}{\partial t} = \frac{\rho_m^2}{\theta}\frac{\partial}{\partial W}\left(\frac{D_i^{\mathrm{S}} A^2}{\theta}\frac{\partial C_i^{\mathrm{S}}}{\partial W}\right) + \nu_i r^{\mathrm{S}} - \frac{C_i^{\mathrm{S}}}{\theta}\frac{\partial \theta}{\partial t} \tag{2}$$

$$\frac{\partial \theta}{\partial t} = \sum_j V_{\mathrm{m},j}\left(\rho_m^2 \frac{\partial}{\partial W}\left(\frac{D_i^{\mathrm{S}} A^2}{\theta}\frac{\partial C_j^{\mathrm{S}}}{\partial W}\right) + \nu_j r^{\mathrm{S}}\theta\right) \tag{3}$$

Maxwell–Stefan approach

Use of a thermodynamic correction factor in Fick's law of diffusion provides a better description of diffusion rates in non-ideal systems, but does not remove the assumption of negligible molar average velocity of the mixture. An alternative and more general treatment of multicomponent mass transfer employs the *generalized Maxwell–Stefan equations*.

When the chemical potential is the only driving force, the force balance in the mass coordinate system may be written as shown in Eq. (4). Since molar quantities are not well defined for cross-linked polymers, the friction forces are here assumed to be proportional to volume fractions. It should be noted that the species velocities are evaluated relative to the polymer mass. The bootstrap relation is obtained from the fact that the velocity of the polymer with respect to itself is zero, *i.e.* $u_{N+1}^{\mathrm{W}} = 0$. The index N+1 in the summations refers to the polymer.

$$-\frac{\partial \mu_i}{\partial W} = \frac{\theta^2}{A^2 \rho_{\mathrm{m}}^2} \sum_{\substack{j=1 \\ j \neq i}}^{N+1} \frac{R_{\mathrm{g}} T}{\mathcal{D}_{ij}} \phi_j \left(u_i^{\mathrm{W}} - u_j^{\mathrm{W}} \right) \tag{4}$$

The material balance for a volume element during multicomponent diffusion controlled volume changes may be written as in Eqs. (5) and (6). The molar fluxes are obtained from a set of force balance equations by using the usual methods of linear algebra.

$$\frac{\partial C_i^{\mathrm{S}}}{\partial t} = \frac{\rho_{\mathrm{m}}}{\theta} \frac{\partial \left(N_i A \right)}{\partial W} + \nu_i r^{\mathrm{S}} - \frac{C_i^{\mathrm{S}}}{\theta} \frac{\partial \theta}{\partial t} \tag{5}$$

$$\frac{\partial \theta}{\partial t} = \sum_{j=1}^{N} V_{\mathrm{m},j} \left(\rho_{\mathrm{m}} \frac{\partial \left(N_j A \right)}{\partial W} + \nu_j r^{\mathrm{S}} \right) \tag{6}$$

Estimates for the liquid–liquid Maxwell–Stefan diffusivities were calculated with the interpolation formula shown in Eq. (7) [8].

$$\mathcal{D}_{ij} = \left(D_i^0 \right)^{\frac{1-\phi_i+\phi_j}{2}} \left(D_j^0 \right)^{\frac{1+\phi_i-\phi_j}{2}} \tag{7}$$

Linear driving force approximation

In the solid phase linear driving force approximation (LDF), the diffusion driving force is approximated by the departure of the average concentration in the particle from phase equilibrium, rather than by evaluating the local concentration gradient at the particle surface. In the case of volume changes of the particles, the temporal derivative of the average solid phase concentration becomes as shown in Eq. (8). An over-bar implies a quantity averaged over the particle volume, and a hat denotes a quantity evaluated at the particle surface in equilibrium with the liquid phase.

$$\frac{\partial \overline{C}_i^{\mathrm{S}}}{\partial t} = \frac{60 \overline{D}_i}{d_{\mathrm{p}}^2} \left(\hat{C}_i^{\mathrm{S}} - \overline{C}_i^{\mathrm{S}} \right) + \nu_i \overline{r}^{\mathrm{S}} - \frac{\overline{C}_i^{\mathrm{S}}}{\overline{\theta}} \frac{\partial \overline{\theta}}{\partial t} \tag{8}$$

$$\frac{\partial \overline{\theta}}{\partial t} = \frac{\rho_{\mathrm{m}}}{W_{\mathrm{p}}} \sum_j V_{\mathrm{m},j} 10 \pi d_p \overline{D}_j \left(\hat{C}_j^{\mathrm{S}} - \overline{C}_j^{\mathrm{S}} \right) + \overline{\theta} \overline{r}^{\mathrm{S}} \sum_j \nu_j V_{\mathrm{m},j} \tag{9}$$

LDF approximation in the Maxwell–Stefan formalism

The linear driving force model may also be interpreted such that mass transfer in the particle occurs across a hypothetical film that comprises the relevant properties of the solid phase. When the finite difference form of the Maxwell–Stefan model (*i.e.,* Eq. (4) with $\partial \mu / \partial W \approx \Delta \mu / \Delta W$) is applied to diffusion across such a film, one obtains Eq. (10). A tilde denotes a mean value in the film. Eqs. (10) – (12) together will be here referred to as LDFMS model.

$$-\frac{\overline{\mu}_i^{\mathrm{S}} - \hat{\mu}_i^{\mathrm{S}}}{R_{\mathrm{g}} T} = \frac{d_{\mathrm{p}}}{10} \sum_{\substack{j=1 \\ j \neq i}}^{N+1} \frac{\tilde{\phi}_j V_{\mathrm{m},i}}{\tilde{\phi}_i \mathcal{D}_{ij} \left(\tilde{\phi} \right)} N_i - \frac{d_{\mathrm{p}}}{10} \sum_{\substack{j=1 \\ j \neq i}}^{N} \frac{V_{\mathrm{m},j}}{\mathcal{D}_{ij} \left(\tilde{\phi} \right)} N_j \tag{10}$$

$$\frac{\partial \bar{C}_i^{\mathrm{S}}}{\partial t} = \frac{\rho_{\mathrm{m}}}{W_{\mathrm{p}}\bar{\theta}} N_i a + \nu_i r^{\mathrm{S}} - \frac{\bar{C}_i^{\mathrm{S}}}{\bar{\theta}} \frac{\partial \bar{\theta}}{\partial t} \tag{11}$$

$$\frac{\partial \bar{\theta}}{\partial t} = \frac{\rho_{\mathrm{m}}}{W_{\mathrm{p}}} \sum_{j=1}^{N} N_j a V_{\mathrm{m},j} + \bar{\theta}\bar{r}^{\mathrm{S}} \sum_j \nu_j V_{\mathrm{m},j} \tag{12}$$

Effect of extent of swelling on the diffusion coefficients

The extent of swelling of an ion-exchange resin affects the mesh width of the free space as well as the tortuosity of the polymer network. Extensive experimental investigation of sorption kinetics is beyond the scope of the present work, and a simple correlation is desired. For this purpose the obstruction model shown in Eq. (13) was chosen. The model is based on that proposed by Mackie and Meares [9] for describing diffusion of electrolytes in ion-exchange membranes.

$$D_i^{\mathrm{S}} = D_i^{\mathrm{S,ref}} \left[\left(1-\phi_{\mathrm{p}}\right) \Big/ \left(1+\phi_{\mathrm{p}}\right) \right]^2 \tag{13}$$

Since the original model does not take account of size or shape of the diffusing species, it only applies to homogeneous materials with a large mesh width relative to the hydrodynamic diameter of the diffusing species. The reference state in the original model is free liquid. In this work, however, the reference state was chosen as a hypothetical, infinitely dilute solution with respect to the polymer, and the diffusion coefficients in the reference state, $D_i^{\mathrm{S,ref}}$, are regarded as adjustable parameters. The lattice model used by Mackie and Meares in the derivation of the model lends itself readily to the Maxwell–Stefan approach as well. The correlation in Eq. (13) is therefore used in both the Fickian diffusion model and the Maxwell–Stefan equations. In the latter case, the Fickian diffusion coefficients are replaced with the Maxwell–Stefan diffusivities $\mathcal{D}_i^{\mathrm{S}}$ and $\mathcal{D}_i^{\mathrm{S,ref}}$.

Boundary conditions for particle diffusion models

The liquid film mass transfer resistance was neglected in the calculations. The boundary condition at the particle surface was therefore obtained from sorption isotherms of the liquid components (see ref. [10] for sorption and swelling data and correlation). A condition of zero flux through the center of the particle yields boundary conditions $\partial C_i^{\mathrm{S}} / \partial W = 0$ and $\partial \theta / \partial W = 0$

Results and discussion

The applicability of the diffusion models presented above was tested with data obtained from non-reactive experiments with water–acetic acid mixtures. The shrinking and swelling of CS16G(H^+) as the external phase is changed from water to a 50 mol-% aqueous acetic acid mixture and vice versa are displayed in Figure 1. The swelling ratio is plotted against a modified time variable in order to enable comparison of the results with particles of different size.

When focusing first on the shrinking data, it is observed that the swelling ratio decreases rapidly, passes through a minimum, and increases slowly towards the new

equilibrium level. The existence of the minimum is due to the relatively large difference in the diffusivities of water and acetic acid: the volumetric flux of water out of the resin is larger than that of the acid into the resin. At the minimum, the volumetric fluxes of the two species have become equal. Swelling dynamics of the CS16G when moving from 50 mol-% water–HOAc mixture to pure water shows opposite behavior – there exists a maximum in the extent of swelling.

The data in Figure 1 also shows that the final state is attained more slowly during shrinking than swelling. This phenomenon was already observed in the early works with ion-exchange resins and other cross-linked polymers [11, p. 293]. Since shrinking starts from the surface of the particle, the solvents have to diffuse through a dense region, the thickness of which only increases with time.

The calculated shrinking and swelling kinetic curves are plotted in Figure 1 and the diffusion coefficient values at the reference state used in the calculations are given in Table 1.

As seen in Figure 1, all models are capable of reproducing the basic shape of the curves but, as expected, the particle diffusion models perform better than the linear driving force approximations. The Maxwell–Stefan approach yielded a higher index of determination (R^2 = 98.9) than the Fickian model (R^2 = 94.0). As usual, the LDF and LDFMS models underestimate the diffusion rates at the early stages of the process, but approach the

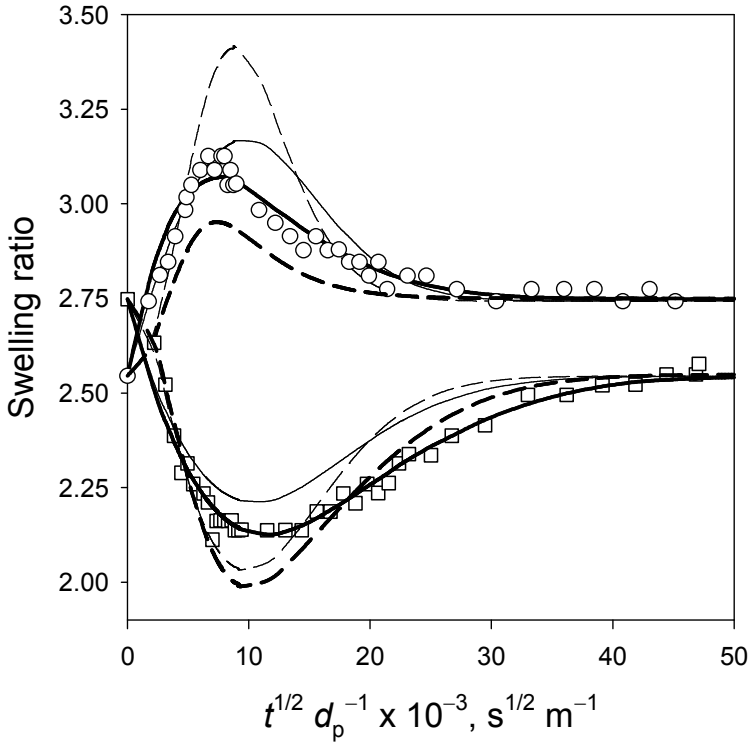

Figure 1. Swelling and shrinking kinetics of CS16G(H^+) at room temperature. Initial and final states: 50 mol-% HOAc–water mixture and pure water. Initial particle size: (○) 984 □m; (□) 903 □m. Solid lines are calculated with particle diffusion models using Fick's law (——) and the generalized Maxwell–Stefan equations (▬▬). Dashed lines are calculated with the approximate LDF (— —) and LDFMS (▬ ▬) models.

Table 1. Fickian ($D_i^{\mathrm{S,ref}}$) and Maxwell–Stefan ($\mathit{Đ}_{i,p}^{\mathrm{S,ref}}$) diffusion coefficients at the reference state of water and acetic acid in CS16G(H^+). Estimated from swelling and shrinking data in Figure 1.

Diffusant	$D_i^{\mathrm{S,ref}}$, $m^2\ s^{-1}$	$\mathit{Đ}_{i,p}^{\mathrm{S,ref}}$, $m^2\ s^{-1}$
Water	$3.3\cdot10^{-9}$	$2.6\cdot10^{-9}$
Acetic acid	$8.5\cdot10^{-10}$	$1.9\cdot10^{-10}$

equilibrium state sooner than the particle diffusion models. The LDF model predicts larger changes in the extent of swelling than the Fickian model in both shrinking and swelling experiments. In fact, a volume-average swelling ratio of 3.5, predicted by the LDF model, is hardly physically realistic for the CS16G resin under any conditions.

The LDFMS model (*i.e.*, Maxwell–Stefan formalism applied to the LDF approximation) predicts considerably lower swelling ratios than the LDF model in the swelling experiment, but only slightly lower swelling ratios at the minimum in the shrinking experiment. This may appear surprising at first sight, especially recalling that the minima and maxima in the volume change data stem from differences in the diffusion rates of the liquids, and considering that the ratio of the $\mathit{Đ}_{i,\mathrm{p}}^{\mathrm{S,ref}}$ values of water and HOAc is more than three times larger than that of the corresponding $D_i^{\mathrm{S,ref}}$ values (see Table 1). The explanation is that the Maxwell–Stefan model accounts for the finite expansibility of the polymer network through the chemical potential of the diffusants.

Conclusions

Mathematical models for coupled diffusion and reaction in swelling and shrinking polymer particles were written without employing the equations of motion. Polymer mass coordinates were used as the frame of reference. Two particle diffusion models based on the Fick's law of diffusion and the generalized Maxwell–Stefan approach, as well as two-point approximations of these, were compared.

It was shown that diffusion induced swelling and shrinking of ion-exchange resin particles is best described with a model based on the Maxwell–Stefan approach because it takes the finite expansibility of the polymer network into account. The LDF model predicted unrealistically large swelling of the resin.

Nomenclature

A	cross-sectional area, m^2
a	surface area to volume ratio, m^{-1}
C^{S}	resin phase concentration, mol m^{-3}
D	Fickian diffusion coefficient, $m^2\ s^{-1}$
$\mathit{Đ}$	Maxwell–Stefan diffusion coefficient, $m^2\ s^{-1}$

d_p particle diameter, m
N flux, mol m^{-2} s^{-1}
R radial coordinate, m
R_g gas constant, J mol^{-1} K^{-1}
r reaction rate, mol m^{-3} s^{-1}
T temperature, K
t time, s
u^w species velocity, kg s^{-1}
V_m molar volume, m^3 mol^{-1}
W mass coordinate, kg
W_p mass of a single resin particle, kg

ϕ volume fraction, –
μ chemical potential, J mol^{-1}
ν stoichiometric coefficient, –
ρ_m density of the polymer, kg m^{-3}
θ swelling ratio, –

References

1. Tanaka, T., Hocker, L., Benedek, G. B., Spectrum of Light Scattered from a Viscoelastic Gel, J. Chem. Phys., 59(1973), 5151-5159
2. Tanaka, T., Fillmore, D. J., Kinetics of Swelling of Gels, J. Chem. Phys., 70(1979), 1214-1218
3. Carbonell, R. G., Sarti, G. C., Coupled Deformation and Mass-Transport Processes in Solid Polymers, Ind. Eng. Chem. Res., 29(1990), 1194-1204
4. El Afif, A., Grmela, M., Non-Fickian Mass Transport in Polymers, J. Rheol., 46(2002), 591-628
5. Billovits, G. F., Durning, C. J., Polymer Material Coordinates for Mutual Diffusion in Polymer–Penetrant Systems, Chem. Eng. Commun. 82(1989), 21-44
6. Bisschops, M. A. T., Luyben, K. C. A. M., van der Wielen, L. A. M., Generalized Maxwell-Stefan Approach for Swelling Kinetics of Dextran Gels, Ind. Eng. Chem. Res., 37(1998), 3312-3322
7. Sainio, T., Tiihonen, J., Paatero, E., Mass Transfer Coupled With Volume Changes in Ion-Exchange Resin Beads, IEX 2004 conference, 4.–7.7.2004, Cambridge, England
8. Xu, X., Cui, Z. F., Modeling of the Co-Transport of Cryoprotective Agents in Porous Medium as a Model Tissue, Biotechnol. Progr., 19(2003), 972-981
9. Mackie, J. S., Meares, P., The Diffusion of Electrolytes in a Cation-Exchange Resin Membrane. I. Theoretical., Proc. Roy. Soc. (London). A232(1955), 498-509
10. Sainio, T., Ion-Exchange Resins as Stationary Phase in Reactive Chromatography, Diss. Lappeenranta University of Technology, Acta Universitatis Lappeenrantaensis 218, Lappeenranta, 2005
11. Helfferich, F., *Ion-exchange*, Dover Publications, New York, 1995